CT-PET Landmark-based Registration Using a Dynamic Lung Model

A. Moreno[1], S. Chambon[1], A. P. Santhanam[2,3], J. P. Rolland[2], E. Angelini[1], I. Bloch[1]
[1] ENST, GET - Télécom Paris, CNRS UMR 5141 LTCI - Paris, France
[2] ODALab, University of Central Florida
[3] Department of Radiation Oncology, MD Anderson Cancer Center Orlando, USA
Antonio.Moreno,Sylvie.Chambon,Isabelle.Bloch,Elsa.Angelini@enst.fr
anand,jannick@odalab.ucf.edu

Abstract

This paper deals with the problem of non-linear landmark-based registration of CT and PET images of thoracic regions. We propose a general method to introduce a breathing model in a registration procedure in order to guarantee physiologically plausible deformations. Initial results are very promising and demonstrate the interest of this method to improve the combination of anatomical and functional images for diagnosis and oncology applications.

1. Introduction

Registration of multimodal medical images is a widely addressed topic and is important in many different domains, in particular for oncology and radiotherapy applications. We consider Computed Tomography (CT) and Positron Emission Tomography (PET) in thoracic regions, which provide complementary information about the anatomy and the metabolism of human body (see Figure 1). Their registration has a significant impact on improving medical decisions for diagnosis and therapy [6]. Linear or affine registration is not sufficient to cope with the local deformations produced by cardiac and respiratory motions. Therefore, non-linear registration methods are required to register multimodality images of thoracic and abdominal regions, even with combined PET/CT [19].

Most of the existing non-linear registration methods use intensity information or features in order to calculate the transformation between the images [7, 12, 22]. Thus they have to either find the transformation that maximises the similarity between the registered image and the target image (iconic methods) or compute a transformation that matches some particular features (landmarks) in both images (geometrical methods). In the case of landmark-based methods, the selection of these particular features is an important task. In many of these methods, the curvature of the surfaces to register is used. However, in most of them, the selection of the landmarks is not studied and detailed [3, 14]. Moreover, most registration methods are based on image information, but do not take into account any physiology of the human body. However, physiological information can be useful in order to ensure realistic deformations and to guide the registration process. While several papers present breathing models built for medical vizualisation [23], but no paper exploits such a model in a registration process. Consequently, in this paper, we propose an approach in which we integrate a physiologically driven breathing model in a non-linear registration procedure based on landmarks in order to guarantee physiologically plausible deformations.

In Section 2, we summarize existing works which use breathing models combined (or not) with registration algorithms and then we provide an overview of the selected model. The proposed model-based non-linear registration algorithm is detailed in Section 3. Then, the application of a landmark-based registration method adapted to pathological cases combined with the breathing model is described in Section 4. Section 5 discusses some results.

Two CT images corresponding to different instants of the breathing cycle

PET image

Figure 1. Equivalent coronal views of the same patient.

2 Breathing Models

2.1 Thoracic Imaging Registration

In this paper we focus on thoracic image registration and more specifically on breathing models that can be applied

to registration of lung images. Different bio-mathematical formulations of the respiratory mechanics that describe the human lung have been developed since the middle of the XX^{th} century [9]. A recent study highlighted the effects of breathing during non-rigid registration process and the importance of taking it into account [20]. There are two main approaches to take into account breathing [11]: develop a mathematical model or employ an empirical algorithm. A third approach exploits the Pressure-Volume (PV) relation in a physically-based model. *Mathematical tools* can be employed to estimate the breathing motion artefacts. The most popular technique is called NCAT (NURBS-based cardiactorso). This model is based on Non-Uniform Rational B-Spline (NURBS) for CT scans of actual patients. It has been proposed in order to correct respiratory artifacts of SPECT images [18]. Rohlfing *et al.* [13] used NURBS in a multi-resolution registration approach based on normalized mutual information for 4D Magnetic Resonance Imaging (MRI). *Empirical models* use external measurements in order to adapt radiation protocols to the tumor's motion. These techniques are not proposed for registration and are dedicated to specific equipments [8]. *Physically-based models* estimate a physical model which is based on the important role of airflow inside the lungs. Many of these methods are based on Active Breathing Coordinator (ABC) [17] and introduce a PV relation [23].

Finally, Rohlfing *et al.* [13] and Sundaram *et al.* [20] proposed to register MRI in order to estimate the breathing model. From a modeling point of view, physically-based deformation methods are suitable for simulating lung dynamics as they allow the precise generation of intermediate 3D lung shapes. These models are easier to adapt to individual patients, without the need of physical external adaptations for each treatment as in the case of empirical models.

2.2 Physics-Based Dynamic 3D Surface Lung Model

An approach for physics and physiology-based modeling of 3D lung dynamics was previously discussed in [15]. The components involved in the modeling and visualization efforts include:

(1) the parameterization of PV data of a human subject which act as an active breathing coordinator for the lung dynamics;
(2) the estimation of the deformation operator from both 4D CT lung data and two 3D CT lung data sets;
(3) the optimisation of the computation in GPU (Graphic Processing Unit) for real-time purposes.

It is to be noted that while items (1) and (2) of the methodology are critical to the registration of PET and CT, item (3) is only reported here for completeness but is not required for the applied problem of this paper. Returning to detailing (2), the deformation operator is computed as follows: The computation takes as inputs the nodal displacements of the 3D lung models and the estimated amount of applied force. The displacements have been shown to be obtained from either 4D or a pair of 3D CT data sets of a normal human subject [16]. The estimated amount of applied force on each node that represents the air-flow inside lungs is estimated based on the lung's orientation with respect to the gravity that controls the air flow. The validation of the lung deformations using 4D-CT datasets were detailed in [16].

3 Using the Breathing Model in Registration

We have conceived an original algorithm in order to introduce the advantages of using the breathing model described above in a registration procedure. Figure 2 shows the computational workflow of the complete algorithm. The inputs consist of one PET volume and two CT volumes of the same patient, corresponding to two different instants of the breathing cycle (intermediate expirations). The first step of the algorithm consists in segmenting the lungs (and, eventually, the tumors) on the PET data and on the two CT data sets, using a robust mathematical-morphology-based approach [4] and meshes (called CT mesh and PET mesh) corresponding to the different segmentation results are computed. The subsequent steps are detailed next.

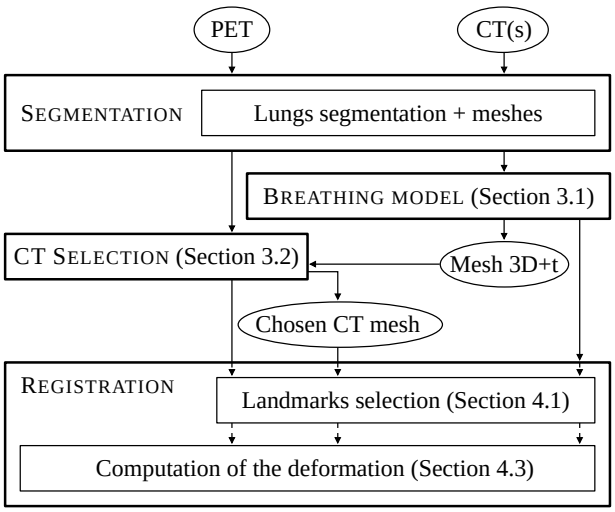

Figure 2. Computational workflow of the algorithm for registration of CT and PET images using a breathing model.

3.1 Computation of a Patient-Specific Breathing Model

With respect to CT-PET registration, we estimate a deformation operator from two CT data sets (i.e. intermediate

expirations) collected with breath-hold maneuver. The displacements of the surface lung vertices can be estimated by using the direction of displacement computed using 4D CT datasets of normal human subjects. This methodology is further detailed in [15].

3.2 CT Selection

By applying the continuous breathing model, we can obtain different instants ("snapshots") of the breathing cycle, generating simulated CT meshes. By comparing each CT mesh with the PET mesh, we select the "closest" one. Let us denote the CT simulated meshes by M_1, M_2,..., M_N. The mesh M_N corresponds to the CT in maximum inhalation and M_1 to maximum exhalation. By using the breathing model, the transformation $\phi_{i\,j}$ between any two instants i and j of the breathing cycle can be computed as: $M_j = \phi_{i\,j}(M_i)$. We compare these CT meshes with the PET mesh (M_{PET}) by means of different criteria. We define a measure of similarity between meshes (or their corresponding volumes) and the mesh that minimizes the chosen criterion (C) is denoted as M_G (for Good):

$$M_G = \arg\min_i C(M_i, M_{PET}). \tag{1}$$

The Root Mean Square (RMS) distance has been chosen as the criterion C, as a first approach:

$$D_{RMS}(M, A) = \sqrt{\frac{1}{2}[d_{RMS}(M, A)^2 + d_{RMS}(A, M)^2]}$$

with $d_{RMS}(M, A) = \sqrt{\frac{1}{|M|}\sum_{p\in M} D(p, A)^2}$ and where $D(p, A) = [\min_{q\in A} d(p, q)]$ with d the Euclidean distance.

3.3 Deformation of the PET

A *direct* registration can be computed between M_{PET} and the original CT mesh M_N (dashed line in Figure 3):

$$M^{Rd}_{PET} = f^{Rd}(M_{PET}, M_N), \tag{2}$$

where f^{Rd} denotes the transformation that registers directly M_{PET} and M_N, and M^{Rd}_{PET} the result of registering the PET directly to the CT mesh M_N. The transformation f^{Rd} may be computed by any registration method adapted to the problem. As an illustrative example, we choose the original CT to correspond to the end-inspiration CT, M_N, but a similar process could be applied for any CT image. In this *direct* approach the deformation itself is not guided by any anatomical knowledge. In addition, if the PET and the original CT are very different (end-inspiration CT), it is likely that this registration procedure will provide physically unrealistic results.

To avoid such potential problems, we propose here an alternative approach: once the appropriate CT (M_G) is selected, we compute the registration between the M_{PET} mesh and the M_G mesh as:

$$M^r_{PET} = f^r(M_{PET}, M_G), \tag{3}$$

where f^r is the registration transformation and M^r_{PET} denotes the registered mesh. Then, the transformation due to the breathing is used to register the M^r_{PET} to the original CT (continuous line in Figure 3). The transformation due to the breathing between M_G and M_N can be computed as the following composition:

$$\Phi_{GN} = \phi_{N-1\,N} \circ \ldots \circ \phi_{G+1\,G+2} \circ \phi_{GG+1}. \tag{4}$$

We apply to M^r_{PET} the same transformation Φ_{GN} in order to compute the registration with M_N:

$$M^{Rbm}_{PET} = \Phi_{GN}(M^r_{PET}) = \Phi_{GN}(f^r(M_{PET}, M_G)), \tag{5}$$

where M^{Rbm}_{PET} denotes the PET registered mesh using the breathing model.

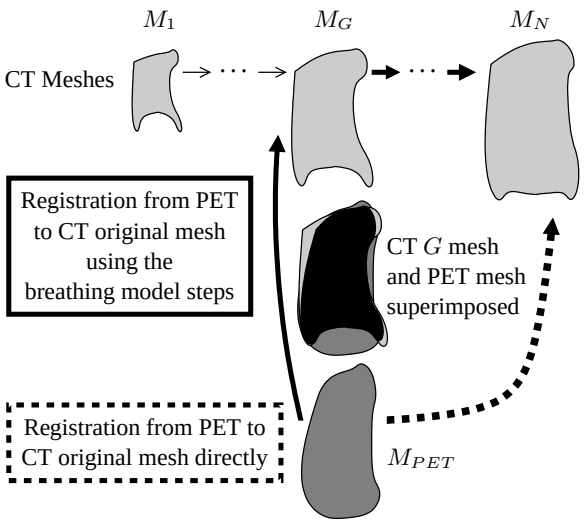

Figure 3. The mesh M_G is the closest to the mesh M_{PET}. We can register it to the (original) CT M_N mesh following one of the two paths (notations are defined in Section 3.3).

4 Registration Adapted to Pathologies

The algorithm described in Section 3 can be applied with any type of registration method. We show here how the proposed approach can be applied for landmark-based registration of multimodality images in pathological cases, in particular for diagnosis, follow-up and radiotherapy treatments.

4.1 Landmark selection and study of their influence

Features selection is an important task in registration. In this section, we focus on voxel selection but more complex features can be detected [1]. The selection can be manual (as in most methods) [21], semi-automatic [14], or automatic [14]. Manual selection is tedious and time-consuming. The authors in [5] suggest that semi-automatic selection is interesting because the knowledge of experts can be integrated in an automatic process. Automatic selection permits reduced execution time with high accuracy. Most of these automatic methods exploit curvature [14]. In [3], an auto-correlation method is also combined with curvature.

In the present work, landmark selection is automatic and based on Gaussian and mean curvatures, according to the following steps:

(1) compute curvature for each voxel of the lung surface;
(2) sort voxels in decreasing order of curvature;
(3) select local maxima (detailed in the following paragraph);
(4) if a uniform selection is needed then add voxels with zero-curvature in the area where no voxels have been considered as landmark.

This algorithm is proposed in order to select particular voxels that provide relevant information. Moreover, we intend to obtain an approximately uniform selection to take into account the entire surface of the lungs for computing the deformation. In step 3, we consider $\mathcal{V} = \{\mathbf{v}_i\}_{i=0..N}$, the set of voxels in decreasing order of curvature, where N is the number of voxels of the surface and $\mathcal{V}_\mathcal{L} = \{\mathbf{v}_{\mathcal{L}i}\}_{i=0..N_\mathcal{L}}$, the set of landmarks, where $N_\mathcal{L}$ is the number of landmarks. For each voxel $\mathbf{v}_i \in \mathcal{V}$ (for $i = 0$ to N) with non-zero-curvature, we add $\mathbf{v}_i$ in $\mathcal{V}_\mathcal{L}$, if $\forall\ \mathbf{v}_j \in \mathcal{V}_\mathcal{L}$, $d_g(\mathbf{v}_i, \mathbf{v}_j) > T$ where d_g is the geodesic distance on the lung surface and T is a threshold to be chosen. With this selection process, some regions (as the most flat ones) may contain no landmark, hence the addition of step 4: for each voxel on the surface of the lung $\mathbf{v}_i \in \mathcal{V}$ and with zero-curvature, if there is no voxel $\mathbf{v}_j \in \mathcal{V}_\mathcal{L}$ with $d_g(\mathbf{v}_i, \mathbf{v}_j) < T$, we add $\mathbf{v}_i$ in $\mathcal{V}_\mathcal{L}$.

Four variants are tested:

(1) MEA – Mean curvature without step 4;
(2) GAU – Gaussian curvature without step 4;
(3) MEA-GAU – Using mean and Gaussian curvature without step 4;
(4) MEA-GAU-UNI – Using mean and Gaussian curvature with step 4.

When mean and Gaussian curvatures are employed (methods MEA-GAU and MEA-GAU-UNI), the set $\mathcal{V}$ merges the set of voxels in decreasing order of mean curvature and the set of voxels in decreasing order of Gaussian curvature. These strategies for landmark selection are compared in Figure 4. Results given by the MEA and GAU methods are different, and it is interesting to combine them (see the results obtained with the MEA-GAU method). The MEA-GAU-UNI method permits to add some points in locally flat regions (see Figure 4).

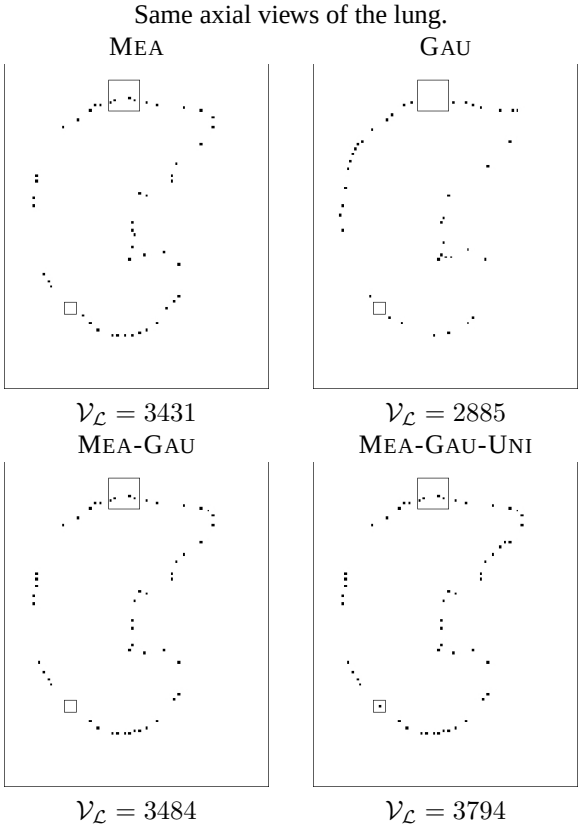

Figure 4. Selection of landmarks – In each images, the same regions are highlighted in small rectangles (and respectively in large rectangles). In the areas surrounded by a large rectangle, there is no landmark with GAU method whereas there are four landmarks with the MEA method. In the fusion method (MEA-GAU), these landmarks are selected. In the areas surrounded by a small rectangle, no landmark is selected with the mean and/or the Gaussian curvatures. However, a landmark is added in this area with the MEA-GAU-UNI method.

4.2 Registration with Rigidity Constraints

We have developed a registration algorithm for the thoracic region in the presence of pathologies [10]. The advantage of our approach is that it takes into account the

tumors, while preserving continuous smooth deformations. We assume that the tumor is rigid and thus a linear transformation is sufficient to cope with its movements between CT and PET images. This hypothesis is relevant and in accordance with the clinicians' point of view, since tumors are often compact masses of pathological tissue. The registration algorithm relies on previously segmented structures (lungs and tumors). Landmarks corresponding to homologous points are defined in both images, and will guide the deformation of the PET image towards the CT image. The deformation at each point is computed using an interpolation procedure based on the landmarks, the specific type of deformation of each landmark (depending on the structure it belongs to), and weighted by a distance function, which guarantees that the transformation is continuous. We have shown that a consistent and robust transformation is obtained [10].

4.3 Registration with Rigidity Constraints and Breathing Model

Once the different CT meshes are computed and the closest CT mesh, M_G, is selected, the PET and the original CT (in our example M_N), are registered as follows:

(1) Select landmarks on the CT mesh M_G (with Gaussian and mean curvatures);
(2) Estimate corresponding landmarks on the PET (using the Iterative Closest Point (ICP) algorithm is involved [2]);
(3) $i = G$;
(4) Track landmarks from M_i to the next CT mesh M_{i+1};
(5) If $M_{i+1} = M_N$, go to step (6) else go to step (4) with $i = i + 1$;
(6) Register (with the method summarized in Section 4.2) the PET and the original CT using the estimated correspondences.

5 Results and Discussion

In this section we present some results we have obtained using the general methodology described in Section 3 and the registration method summarised in Section 4.

We have applied our algorithm on a normal case and on a pathological case, exhibiting one tumor. In both cases, we have one PET and two CT images. First, the breathing model is computed using the meshes of the segmented lungs. Then, we compare 10 (regularly distributed) instants of the generated model with the PET. Figure 5 shows the results of volume/surface comparison for two instants of the CT: the closest and the end-inspiration.

The results obtained with this algorithm are physically-based and more realistic than results obtained by registering the PET directly with the original CT. First results confirm this statement, as shown in figures of results.

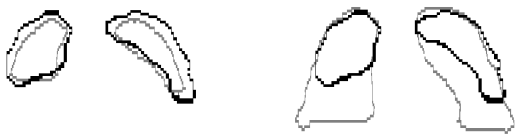

(a) $D_{RMS} = 12.1$ (b) $D_{RMS} = 24.2$

Figure 5. Superimposition of the contours of the PET (black) and the CT lungs (grey) at two instants of the breathing cycle: (a) closest instant M_G, (b) end-inspiration instant M_N.

6 Conclusion and Future Work

We have developed a CT/PET registration method that uses a breathing model to guarantee physiologically plausible deformations. The method consists in computing a deformation guided by a breathing model.

First results on two cases (one normal case and one pathological case) are very promising and show the improvement brought by the breathing model.

In particular, for pathological cases, our algorithm avoids undesired tumor misregistrations and preserves tumor geometry and intensity. Moreover, as the tumor in CT and PET has not necessarily the same size and shape, the registration of these two modalities is very useful because all the information of the PET image is preserved. This is very important in order to know the true extension of the pathology for diagnosis and for the treatment of the tumor with radiotherapy, for example.

In this paper, as a first step we consider the impact of physiology on lung surface deformations from normal human subjects. We are in the process of modeling the impact of changes in the human lung physiology on lung surface deformations according to the lung tumor size and location. Therefore the methodology presented in this paper will further benefit upon the inclusion of patho-physiology once established. Nevertheless, the use of normal lung physiology serves to demonstrate improvements in CT and PET registration using a physics-based 3D breathing lung model. Moreover, future work includes a refined "snapshot" selection, using further subdivisions of time intervals, a more precise characterisation of the tumor movement and its influence on the breathing, and a deeper evaluation on a larger database, in collaboration with clinicians.

References

[1] W. Beil, K. Rohr, and H. Stiehl. Investigation of approaches for the localization of anatomical landmarks in 3D medical images. pages 265–270, Apr. 1997.

[2] P. Besl and N. McKay. A Method for Registration of 3-D Shapes. *IEEE TPAMI*, 14(2):239–256, 1992.

[3] M. Betke, H. Honga, D. Thomasa, C. Princea, and J. Kob. Landmark detection in the chest and registration of lung surfaces with an application to nodule registration. *Medical Image Analysis*, 7(3):265–281, 2003.

[4] O. Camara, G. Delso, O. Colliot, A. Moreno-Ingelmo, and I. Bloch. Explicit Incorporation of Prior Anatomical Information into a Non-Rigid Registration of Thoracic and Abdominal CT and 18-FDG Whole-Body Emision PET Images. *IEEE TMI*, 26(2), 2007.

[5] T. Hartkens, D. Hill, A. Castellano-Smith, D. Hawkes, C. Maurer Jr., A. Martin, W. Hall, H. Liu, and C. Truwit. Using Points and Surfaces to Improve Voxel-Based Non-Rigid Registration. In *MICCAI*, volume 2489, pages 565–572, Tokyo,, 2002.

[6] W. Lavely, C. Scarfone, H. Cevikalp, R. Li, D. Byrne, A. Cmelak, B. Dawant, R. Price, D. Hallahan, and J. Fitzpatrick. Automatic registration of PET and CT studies for clinical use in thoracic and abdominal conformal radiotherapy. *Medical Physics*, 31(5):1083–1092, 2004.

[7] J. Maintz and M. Viergever. A Survey of Medical Image Registration. *Medical Image Analysis*, 2(1):1–36, 1998.

[8] J. McClelland, J. Blackall, S. Tarte, A. Chandler, S. Hughes, S. Ahmad, D. Landau, and D. Hawkes. A Continuous 4D Motion Mmodel from Multiple Respiratory Cycles for Use in Lung Radiotherapy. *Medical Physics*, 33(9):3348–3358, 2006.

[9] J. Mead. Measurement of Inertia of the Lungs at Increased Ambient Pressure. *JAP*, 2(1):208–212, 1956.

[10] A. Moreno, G. Delso, O. Camara, and I. Bloch. Non-linear Registration Between 3D Images Including Rigid Objects: Application to CT and PET Lung Images With Tumors. In *DEFORM*, pages 31–40, 2006.

[11] M. Murphy. Tracking Moving Organs in Real Time. *Seminars in radiation oncology*, 14(1):91–100, 2004.

[12] J. Pluim and J. Fitzpatrick. Image Registration. *IEEE TMI*, 22(11):1341–1343, 2003.

[13] T. Rohlfing, C. Maurer, W. O'Dell, and J. Zhong. Modeling Liver Motion and Deformation During the Respiratory Cycle Using Intensity-Based Free-Form Registration of Gated MR Images. *Medical Physics*, 31(3):427–432, 2004.

[14] K. Rohr, H. Stiehl, R. Sprengel, T. Buzug, J. Weese, and M. Kuhn. Landmark-based elastic registration using approximating thin-plate splines. 20(6):526–534, 2001.

[15] A. Santhanam. *Modeling, Simulation, and Visualization of 3D Lung Dynamics*. PhD thesis, 2006. (Co-advising with Dr. Pattanaik, CS).

[16] A. Santhanam, C. Imielinska, P. Davenport, P. Kupelian, and J. Rolland. Modeling Simulation and Visualization of Real-Time 3D Lung Dynamics. *IEEE TITB*, 2007. In press.

[17] D. Sarrut, V. Boldea, S. Miguet, and C. Ginestet. Simulation of Four-Dimensional CT Images from Deformable Registration between Inhale and Exhale Breath-Hold CT Scans. *Medical Physics*, 33(3):605–617, 2006.

[18] W. Segars, D. Lalush, and B. Tsui. Study of the Efficacy of Respiratory Gating in Myocardial SPECT Using the New 4-D NCAT Phantom. *IEEE TNS*, 49(3):675–679, 2002.

[19] R. Shekhar, V. Walimbe, S. Raja, V. Zagrodsky, M. Kanvinde, G. Wu, and B. Bybel. Automated 3-Dimensional Elastic Registration of Whole-Body PET and CT from Separate or Combined Scanners. *The Journal of Nuclear Medicine*, 46(9):1488–1496, 2005.

[20] T. Sundaram and J. Gee. Towards a Model of Lung Biomechanics: Pulmonary Kinematics Via Registration of Serial Lung Images. *Medical Image Analysis*, 9(6):524–537, 2005.

[21] J. B. West, C. R. Maurer, and J. R. Dooley. Hybrid point-and-intensity-based deformable registration for abdominal ct images. In *SPIE Medical Imaging*, volume 5747, pages 204–211, 2005.

[22] B. Zitovà and J. Flusser. Image Registration Methods: A Survey. *Image and Vision Computing*, 21:977–1000, 2003.

[23] V. Zordan, B. Celly, B. Chiu, and P. DiLorenzo. Breathe Easy: Model and Control of Human Respiration for Computer Animation. *Graphical Models*, 68(2):113–132, 2006.